

Time-dependent climate sensitivity and the legacy of anthropogenic greenhouse gas emissions

Richard E. Zeebe¹

Department of Oceanography, School of Ocean and Earth Science and Technology, University of Hawaii at Manoa, Honolulu, HI 96822

Edited by Robert E. Dickinson, The University of Texas at Austin, Austin, TX, and approved July 9, 2013 (received for review February 8, 2013)

Climate sensitivity measures the response of Earth's surface temperature to changes in forcing. The response depends on various climate processes that feed back on the initial forcing on different timescales. Understanding climate sensitivity is fundamental to reconstructing Earth's climatic history as well as predicting future climate change. On timescales shorter than centuries, only fast climate feedbacks including water vapor, lapse rate, clouds, and snow/sea ice albedo are usually considered. However, on timescales longer than millennia, the generally higher Earth system sensitivity becomes relevant, including changes in ice sheets, vegetation, ocean circulation, biogeochemical cycling, etc. Here, I introduce the time-dependent climate sensitivity, which unifies fast-feedback and Earth system sensitivity. I show that warming projections, which include a time-dependent climate sensitivity, exhibit an enhanced feedback between surface warming and ocean CO₂ solubility, which in turn leads to higher atmospheric CO₂ levels and further warming. Compared with earlier studies, my results predict a much longer lifetime of human-induced future warming (23,000–165,000 y), which increases the likelihood of large ice sheet melting and major sea level rise. The main point regarding the legacy of anthropogenic greenhouse gas emissions is that, even if the fast-feedback sensitivity is no more than 3 K per CO₂ doubling, there will likely be additional long-term warming from slow climate feedbacks. Time-dependent climate sensitivity also helps explaining intense and prolonged warming in response to massive carbon release as documented for past events such as the Paleocene–Eocene Thermal Maximum.

In the context of anthropogenic greenhouse gas (GHG) emissions, equilibrium climate sensitivity is often referred to as the change in Earth's global mean near-surface air temperature (after reaching a new steady state) following a doubling of the atmospheric carbon dioxide (CO₂) concentration. Generally, climate sensitivity may be referred to as the change in global mean near-surface air temperature in response to a forcing, taking into account various processes in the climate system that can either amplify or dampen the response to an initial perturbation (1, 2). These processes are referred to as climate feedbacks, which can operate on very different timescales. In addition, climate sensitivity may depend on the type of forcing and the background climate state (3). In the past, climate sensitivity studies were mostly based on numerical climate models and have focused on the preindustrial/present climate system over timescales of decades to centuries as this approach appeared viable for predicting future climate change (1, 4, 5). However, recent studies emphasize the investigation of past climate changes and the importance of feedback analysis for a more fundamental understanding of climate sensitivity (3, 6–12).

Feedback Analysis

A useful tool for a systematic examination of climate sensitivity is feedback analysis (2, 6, 13), which can be used to disentangle contributions of individual feedbacks to the overall response. For instance, the global surface temperature change (ΔT) following a change in radiative forcing (ΔR_f) may be written as (6):

$$\Delta T = \Lambda_0^{-1} (\Delta R_f + \lambda_1 \Delta T + \lambda_2 \Delta T + \dots), \quad [1]$$

where λ_i are climate feedback parameters. Eq. 1 is based on a linearization around an equilibrium state and says that the system's overall temperature response is composed of a contribution that directly depends on the forcing ΔR_f and additional contributions from feedbacks that depend on ΔT itself (for equilibrium and transient response, see *SI Text*). The Planck feedback parameter Λ_0 represents the change in long-wave radiation ($\propto dT^4/dT$) following adjustment of T required to balance ΔR_f in the absence of other feedbacks ($\Lambda_0 \simeq 3.2 \text{ W}\cdot\text{m}^{-2}\cdot\text{K}^{-1}$; ref. 5). The λ_i are positive here for a positive feedback, i.e., when enhancing the Planck response. The radiative forcing ΔR_f may be due to changes in GHGs, dust, insolation, etc. For example, a doubling of atmospheric CO₂ ($2\times \text{CO}_2$) results in a radiative forcing of $\sim 3.7 \text{ W}\cdot\text{m}^{-2}$ (14). Thus, at $2\times \text{CO}_2$, the global surface temperature increase ($\Delta T_{2\times}$) based on the Planck response alone (all other $\lambda_i = 0$) would be only $\sim 1.2 \text{ K}$. The difference between the Planck response and the likely range for $\Delta T_{2\times}$ of 2–4.5 K (15) is hence due to other feedbacks.

The overall temperature change obtained from Eq. 1 is $\Delta T = \Delta R_f (\Lambda_0 - \sum \lambda_i)^{-1}$ and the climate sensitivity, S , is:

$$S = \frac{\Delta T}{\Delta R_f} = \frac{1}{\Lambda_0 - \sum \lambda_i}. \quad [2]$$

The sensitivity increases for positive feedback parameters ($\lambda_i > 0$, the forcing is amplified) and decreases for $\lambda_i < 0$ (forcing is damped). Considering only fast feedbacks including water vapor, lapse rate, clouds, and snow/sea ice albedo, the fast-feedback sensitivity is $S^{\text{ff}} = (\Lambda_0 - \sum \lambda_i^{\text{ff}})^{-1}$, where λ_i^{ff} are feedback parameters of the fast processes (the typical timescale separating fast and slow processes is often taken as 100 y). Considering fast and slow feedbacks including changes in vegetation, ocean circulation, ice sheets, biogeochemical cycling, etc., the Earth system sensitivity is $S^{\text{es}} = (\Lambda_0 - \sum \lambda_i^{\text{ff}} - \sum \lambda_i^{\text{es}})^{-1}$, where λ_i^{es} are feedback parameters of the slow processes. Below, S and $S_{2\times} = S \times 3.7 \text{ W}\cdot\text{m}^{-2}$ is the climate sensitivity in $\text{K}(\text{Wm}^{-2})^{-1}$ and kelvin per CO₂ doubling, respectively (for more details, see ref. 3).

Time-Dependent Climate Sensitivity

Until present, the fast-feedback and Earth system sensitivity have generally been considered separately because the former operates primarily on timescales of decades, and the latter primarily on millennia or longer. For example, climate sensitivity in general circulation models (GCMs) essentially equals the fast-feedback sensitivity and appears fairly constant on centennial timescale

Author contributions: R.E.Z. designed research, performed research, analyzed data, and wrote the paper.

The author declares no conflict of interest.

This article is a PNAS Direct Submission.

¹To whom correspondence should be addressed. E-mail: zeebe@hawaii.edu.

This article contains supporting information online at www.pnas.org/lookup/suppl/doi:10.1073/pnas.1222843110/-DCSupplemental.

(16, 17) [earlier GCM results suggesting an increase in the effective climate sensitivity (18) over centuries have been considered an artifact (17)]. Climate sensitivity in simple models used for long-term integrations is often prescribed and constant on all timescales. However, a climate sensitivity parameter that provides a transition between fast and slow feedbacks seems to be missing. In nature, no separation between fast-feedback and Earth system sensitivity exists as climate sensitivity simply changes over time, depending on the varying contributions of the feedbacks on different timescales. Hence, I introduce the time-dependent climate sensitivity, $S(t)$:

$$S(t) = \frac{1}{\Lambda_0 - \sum \lambda_i^{\text{ff}} - \sum c_j(t)\lambda_j^{\text{es}}}, \quad [3]$$

where $c_j(t)$ are coefficients that vary between 0 and 1—depending on the characteristic response time of the slow process j [different functional relationships for the $c_j(t)$ are possible] (*Methods* and Fig. 1). Time-dependent climate sensitivity introduced here as a theoretical concept (Eq. 3) should not be confused with

transient ocean heat uptake (16, 19–21) or other seemingly transient effects in climate models (17, 18). The theoretical advance provided by $S(t)$ is that it unifies fast-feedback and Earth system sensitivity because $S(t)$ approaches S^{ff} and S^{es} , respectively, as $c_j \rightarrow 0$ and $c_j \rightarrow 1$. The practical value of $S(t)$ is that it allows evaluation of climate sensitivity continuously over timescales from decades to millions of years. This includes analyses of past climate episodes throughout Earth’s history as well as future predictions of anthropogenic climate change.

Whereas it seems currently difficult to further constrain the fast-feedback sensitivity (5, 22), recent paleoclimate studies provide new constraints on the slow feedbacks (3, 7–10). Below, I use these paleo-constraints to provide future warming projections. Given scenarios of anthropogenic GHG emissions, I have forecast the evolution of future atmospheric GHG concentrations and surface temperature change using $S(t)$ and the Long-term Ocean-atmosphere-Sediment Carbon cycle Reservoir (LOSCAR) model (23) (Fig. 2). Ocean heat uptake efficiency, which is known to delay surface warming over a few centuries (19, 20, 24), was included using an effective heat capacity/surface response time (*SI Text*). Furthermore, slow processes such as changes in vegetation, ice sheets, non-CO₂ GHGs, etc., were taken into account by specifying slow feedback parameters λ_j^{es} and corresponding response times τ_j (*Methods* and Table 1). (The slow feedback from non-CO₂ GHGs in response to warming is not to be confused with the emission of these gases due to anthropogenic activities.) The λ_j^{es} are constrained both directly by a decomposition analysis of climate feedbacks during past climate episodes (3, 10) and indirectly by reconstructions of Earth system sensitivity (3, 7–10) (*Methods*). Moreover, uncertainties in the slow feedbacks are examined by varying the slow-feedback parameters (Fig. 3). Note that carbon release from permafrost and oceanic hydrates is also part of the feedback. However, these processes can be explicitly modeled and included here as carbon sources enhancing radiative forcing (Table 1 and *Methods*), rather than implicitly affecting λ values in a less specific fashion (Eq. 3). The individual contributions of the various processes to future warming projections are discussed below.

The fast-feedback parameters (λ_i^{ff}) entering Eq. 3 were taken such that the fast-feedback sensitivity, $S_{2\times}^{\text{ff}} = 3$ K (Fig. 1). Although 3 K is the most likely value for $S_{2\times}^{\text{ff}}$ (15), there are uncertainties associated with the λ_i^{ff} (2, 5, 15), meaning that $S_{2\times}^{\text{ff}}$ ’s absolute value might be different. However, currently there is little indication from climate models that the λ_i^{ff} vary systematically over centennial timescale (17). In GCMs, the λ_i^{ff} also seem to depend on the type of forcing and the background climate state, yet systematic relationships that can be applied in future projections appear difficult to infer at this stage (3, 25). The present focus is the evolution of the slow feedbacks, whose systematic temporal behavior may be constrained based on recent observations. The present focus is not the uncertainties in the fast feedbacks. For the results presented below, it is important, however, to keep in mind that the calculations are based on the most likely value of $S_{2\times}^{\text{ff}} = 3$ K.

Results and Discussion

The maximum global surface warming in response to a total fossil fuel input of 2,500 Pg C over 500 y is projected at ~ 4 K if ocean heat uptake efficiency and constant climate sensitivity is included (Fig. 2); for other emission scenarios and parameter variations, see below and Fig. 3. This “base case” also includes temperature effects on ocean CO₂ chemistry and increased surface ocean stratification. The surface warming (ΔT) falls below 4 K within $\sim 1,000$ y after reaching its peak value, even if additional GHG emissions and carbon release from permafrost and oceanic hydrates are included (Table 1). However, with a time-dependent $S(t)$ that includes additional slow feedbacks at moderate strength from changes in vegetation, non-CO₂ GHGs,

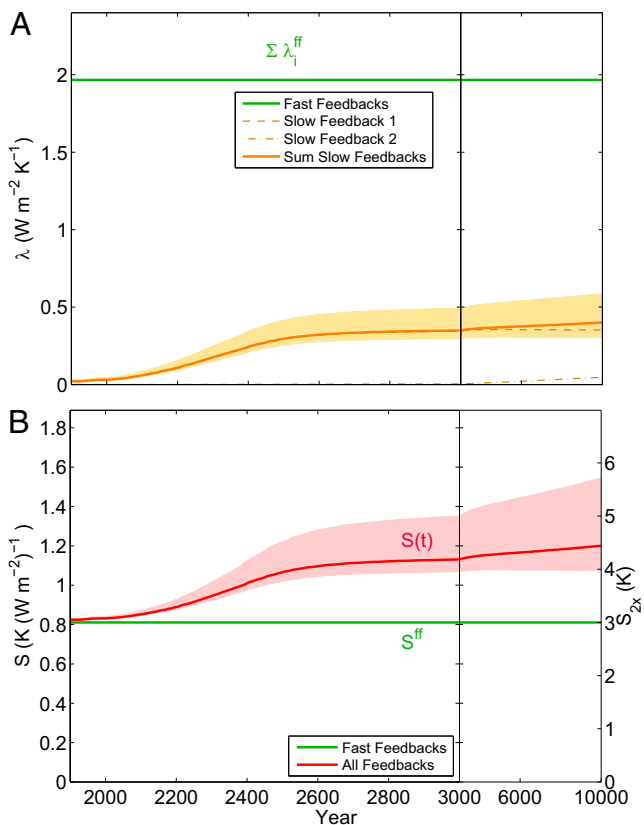


Fig. 1. Illustration of climate feedback parameters and climate sensitivity over time. (A) Fast (λ_i^{ff}) and slow (λ_j^{es}) climate feedback parameters. The sum of the fast-feedback parameters is $\sum \lambda_i^{\text{ff}} = 1.97 \text{ W}\cdot\text{m}^{-2}\cdot\text{K}^{-1}$, yielding a fast-feedback sensitivity of $S_{2\times}^{\text{ff}} = 3.7/(3.2 - 1.97) = 3.0$ K per CO₂ doubling (see text and B). The slow feedbacks are illustrated with $\tau_1 = 200$ y and $\tau_2 = 5,000$ y using Eqs. 3 and 6 (see text and *Methods*), the temperature anomaly of the example shown in Fig. 2B (red graph), and moderate slow-feedback strength (lines labeled “slow”). The shaded error envelopes in A and B were calculated based on the likely range of $\lambda_i^{\text{es}} + \lambda_j^{\text{es}}$ (*Methods* and Fig. 3). Note the nonlinear horizontal time axis. (B) Climate sensitivity in $\text{K}(\text{W}\cdot\text{m}^{-2})^{-1}$ (left axis) and in kelvin per CO₂ doubling (right axis). Considering only fast feedbacks results in a climate sensitivity that is constant over time (S^{ff}). However, including slow, time-dependent feedbacks (A) leads to a climate sensitivity that varies over time [$S(t)$].

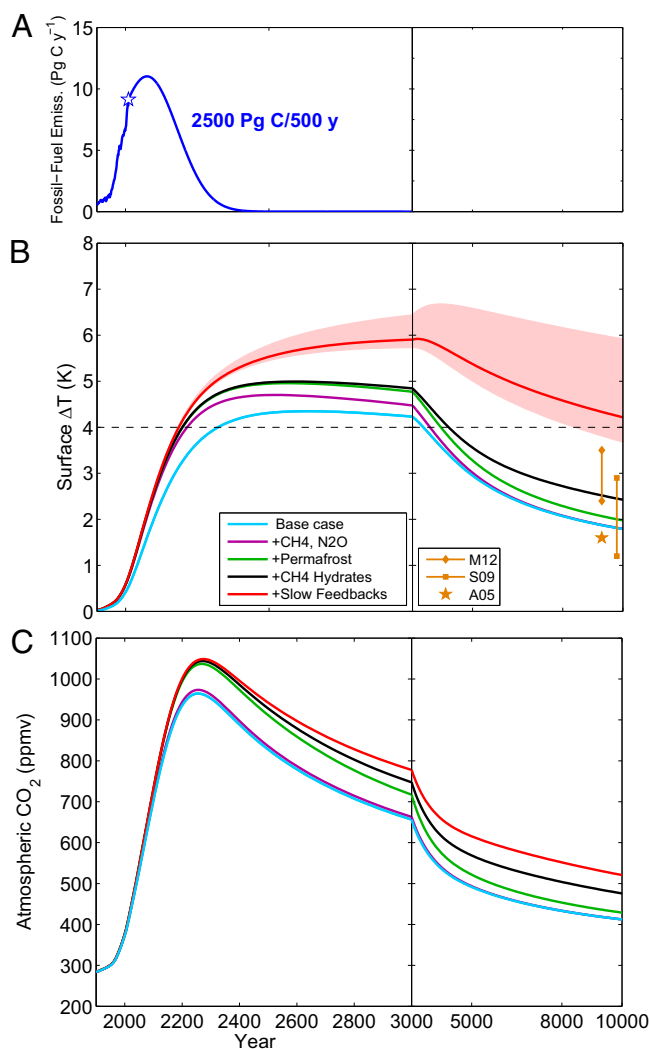


Fig. 2. Example of projected anthropogenic warming including various forcings and feedbacks. (A) Anthropogenic CO₂ emission scenario based on historic emissions until 2010 and a Gauss curve for $t > 2010$ with 2,500 Pg C total integrated emissions (46). (B) Projected global surface warming ($S_{2\times}^{ff} = 3$ K). The base case includes temperature effects on ocean CO₂ chemistry, increased surface ocean stratification, and ocean heat uptake efficiency. Additional processes that can be included explicitly here as forcings include anthropogenic emissions of non-CO₂ greenhouse gases (GHGs), permafrost, and oceanic methane hydrates (Methods). Additional slow feedbacks include combined effects of changes in vegetation, non-CO₂ GHGs, low-latitude glaciers/ice caps, and high-latitude ice sheets. Note: the slow feedback from non-CO₂ GHGs in response to warming is not to be confused with the emission of these gases due to anthropogenic activities. The red graph is based on moderate values for the slow-feedback parameters $\lambda_{1,2}$ (see text and Methods). The shaded error envelope (light red) was calculated based on the likely range of $\lambda_1^{es} + \lambda_2^{es}$ (Methods and Fig. 3). Also shown are warming estimates in Y10,000 from previous studies (orange symbols) that included sediments and a negative, long-term weathering feedback: A05 (2,000 Pg), S09 (1,540/3,720 Pg), M12 (3,000 Pg) = refs. 38, 40, 41 (total C emissions in parentheses; A05's warming pertains to mean ocean warming). (C) Atmospheric CO₂ concentrations corresponding to the projected scenarios in B. Higher atmospheric CO₂ levels for given emissions are due to ocean solubility feedback. Note the nonlinear horizontal time axis.

low-latitude glaciers/ice caps, and high-latitude ice sheets (Methods and Fig. 1), ΔT remains elevated >5 K beyond Y3,000 and >4 K beyond Y10,000 (Fig. 2). Elevated temperatures enhance the feedback between warming and ocean CO₂ solubility, causing higher atmospheric CO₂ levels for given emissions (Fig. 2 A and C) and

Table 1. Processes included as forcings/feedbacks in the present study

Process	Forcing	Feedback	λ
Emissions			
Fossil fuel CO ₂ emissions	✓		—
Anthropogenic CH ₄ , N ₂ O emissions*	✓		—
Climate system			
Fast feedbacks [†]		✓	λ_i^{ff}
Vegetation		✓	λ_1^{es}
Non-CO ₂ GHGs [‡]		✓	λ_1^{es}
Low-latitude ice		✓	λ_1^{es}
High-latitude ice sheets		✓	λ_2^{es}
Carbon cycle			
Permafrost C release	✓	§	—
Hydrate C release	✓	§	—
Ocean CO ₂ solubility [¶]		✓	—
Sediment CaCO ₃ dissolution		✓	—
Weathering		✓	—

*Anthropogenic emissions. Not to be confused with the slow feedback of non-CO₂ GHGs.

[†]Includes changes in water vapor, lapse rate, clouds, and snow/sea ice albedo.

[‡]Slow feedback. Not to be confused with anthropogenic CH₄ and N₂O emissions.

[§]C release from permafrost/hydrates are actually feedbacks but can be included here explicitly as a forcing (Eq. 1), rather than implicitly affecting λ values (less specific).

[¶]Calculated as a function of temperature.

|| Explicitly calculated in carbon cycle model (23).

further warming. If sustained over centuries, prolonged warming of this magnitude increases the likelihood of large ice sheet disintegration and major sea level rise (26, 27) (see below, Eq. 4). In addition, the continued warming may cause higher and extended carbon release from permafrost and oceanic methane hydrates than the estimates included in the present simulations (Fig. 2). It is important that the enhanced long-term warming predicted here is due to slow feedbacks from vegetation, non-CO₂ GHG, and ice rather than slow ocean heat uptake (21), which is included in the simulations but delays warming only on a timescale of centuries (16, 20, 24).

The slow-feedback parameters (λ_j^{es}) may be constrained to a certain range of the parameter space using results from paleo-climate studies (Methods). To sample this parameter space, I have calculated future warming trajectories for various emission scenarios and appropriate values for the λ_j^{es} (Fig. 3). The suite of projection results can be summarized by computing the maximum warming and a mean warming index for each projection i (relevant e.g., for ice sheet melting):

$$W_i = (t_2 - t_1)^{-1} \int_{t_1}^{t_2} \Delta T_i(t) dt, \quad [4]$$

where $\Delta T_i(t)$ is the global surface warming above preindustrial levels; $[t_1, t_2] = [Y2013, Y10000]$. Thus, W_i represents the calculated average future warming from the present until year 10,000. The maximum warming depends only weakly on the slow feedbacks and is hence similar for a given emission scenario (Fig. 3A). However, the average warming, W_i , depends strongly on the slow feedbacks and predominantly measures the longevity of the warming (Fig. 3B). This is because the present simulations show a long warming tail, rather than intense peak warming and rapid cooling (SI Text). Given estimates of Earth system sensitivity (Methods), I predict an increase in the

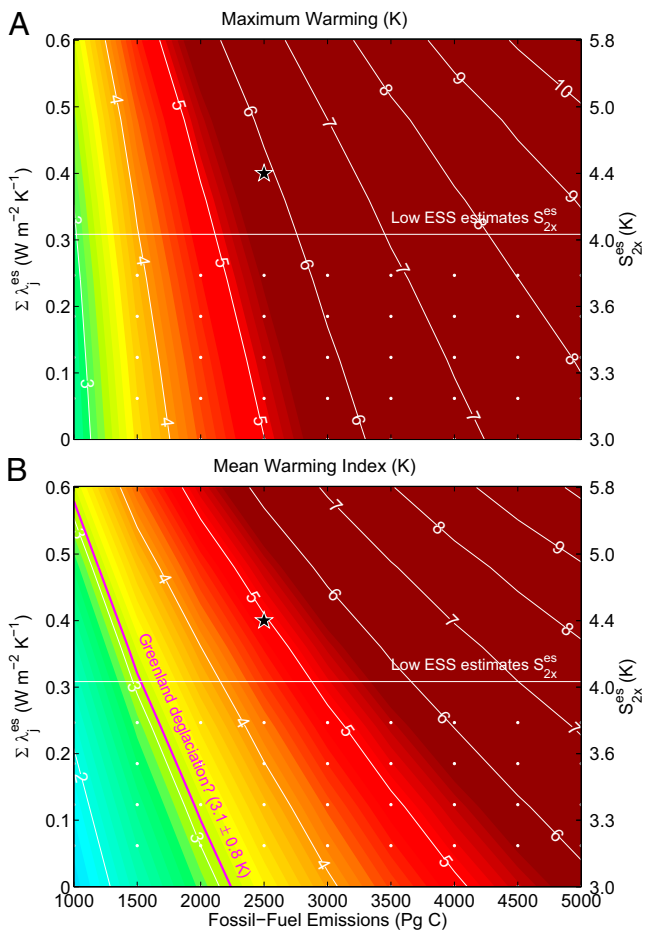


Fig. 3. Summary of projected future warming trajectories. (A) Projected maximum surface warming above preindustrial levels ($S_{2x}^{ff} = 3$ K) as a function of total anthropogenic fossil fuel emissions and slow-feedback parameters (λ_1^{es} and λ_2^{es}). λ_1^{es} represents the combined effects of changes in vegetation, non- CO_2 GHGs, and low-latitude glaciers/ice caps ($\tau_1 = 200$ y); λ_2^{es} represents changes in high-latitude ice sheets ($\tau_2 = 5,000$ y). λ_1^{es} and λ_2^{es} were simultaneously increased to cover the likely range of $\lambda_1^{es} + \lambda_2^{es}$ (Methods). The right vertical axis shows the corresponding Earth system sensitivity, $S_{2x}^{es} = 3.7 \times (\Lambda_0 - \sum \lambda_i^{ff} - \sum \lambda_j^{es})^{-1}$ K. The horizontal line indicates estimates of Earth system sensitivity (ESS) at the lower end of the spectrum (3, 8). Thus, the white-dotted area below that line represents an unlikely parameter space for long-term future warming. (B) Projected mean surface warming index W_i (Eq. 4). The stars indicate parameter values used for the projection shown in Fig. 2 (red graph). The magenta line indicates the warming threshold for the irreversible deglaciation of the GIS of 3.1 ± 0.8 K given in ref. 26.

duration and magnitude of future warming. For instance, at total emissions of 2,500 Pg C and $S_{2x}^{ff} = 3$ K, the likely range of mean warming over the coming millennia is about 4–6 K, rather than ~3.5 K when slow feedbacks are ignored (Fig. 3B). This suggests consequences for long-term future climate change projections.

For example, the warming threshold for irreversible deglaciation of the Greenland ice sheet (GIS) (equivalent sea level rise, ~7 m) has been estimated at 3.1 ± 0.8 K above preindustrial levels (26). A more recent study using a coupled climate-ice sheet model (27) puts this threshold at 1.6 K (range, 0.8–3.2 K). However, at 1.6 K, GIS deglaciation may take $\gg 10^4$ y. The study emphasizes that the timescale of melt depends strongly on the magnitude and duration of the temperature overshoot above the threshold. This feature is better represented here by W_i (Eq. 4) than by the maximum warming. For example, all but one simulation with $W_i > 3.1$ K also include sustained warming $\Delta T > 3.1$ K

for more than 4,000 y (SI Text). To avoid GIS deglaciation, total allowed emissions would be ~2,200 Pg C for a threshold of 3.1 K and $S_{2x}^{ff} = 3$ K if slow feedbacks are ignored (Fig. 3B). However, including slow feedbacks, allowed emissions might be only 1,000–1,700 Pg C (depending on feedback parameters). Humans have already released >365 Pg C from fossil fuel and cement over the past 250 y (28).

Projected Warming Contributions

The fast-feedback response to anthropogenic CO_2 emissions represents the largest contribution to the projected warming over the next few centuries. For the base case (2,500 Pg C/500 y, Fig. 2), the calculated maximum additional warming from anthropogenic CH_4 and N_2O emissions is ~0.6 K, consistent with previous studies (29). Carbon release from permafrost is projected to contribute an additional ~0.3 K at most on centennial timescale. This is a conservative estimate, using a low sensitivity of the permafrost reservoir size to warming (Methods). Over several millennia, carbon release from methane hydrate systems adds another ~0.5 K at maximum to the warming (30). Note that the carbon release from methane hydrates predicted for the future does not imply releases of similar magnitude on glacial-interglacial timescale. This is because (i) the recharge time of the oceanic hydrate reservoir is on the order of millions of years and (ii) the temperature swings during glacial cycles were more pronounced toward colder, rather than warmer conditions. Models that include these features predict a relatively small methane release on deglaciations, in agreement with ice core and deep-sea archives, including stable carbon isotope records (31). Note also that, although the last interglacial period was warmer than the preindustrial era, deep-ocean temperatures appear to have been only slightly elevated (32), preventing significant methane release. The predicted future release is comparatively larger because the magnitude of the anticipated anthropogenic warming is unprecedented over the past several million years (31).

Over the coming millennia, an increasing portion of the additional predicted warming is due to slow feedbacks, which also maintain temperatures at elevated levels over this timescale (Fig. 2) (for variation of the slow feedback strength over a wide range, see Fig. 3). At moderate feedback strength (Methods), the slow feedbacks (mostly vegetation, non- CO_2 GHGs, and low-latitude glaciers/ice caps) cause further warming of about ~1 K by year 3,000 in the simulations, relative to the case including anthropogenic GHGs, permafrost, and hydrates (Table 1 and Fig. 2). By year 10,000, the calculated difference in surface temperature warming between these two cases increases to ~1.8 K mostly due to changes in high-latitude ice sheets, which add to the slow feedback strength on this timescale (Fig. 1).

The implied future changes in high-latitude ice sheets, for example, may be illustrated by comparing feedback parameters (λ values) used in the future projections to those estimated for the Last Glacial Maximum (LGM) to Holocene transition. Note that λ values measure the feedback strength per unit warming, not per absolute warming (Eq. 1). For the moderate future scenario, $\lambda_2^{es} = 0.05 \text{ W}\cdot\text{m}^{-2}\cdot\text{K}^{-1}$ (Methods), whereas for the LGM, λ_2^{es} has been estimated at ~0.70 $\text{W}\cdot\text{m}^{-2}\cdot\text{K}^{-1}$ (3, 10). In other words, in the future projections with moderate slow feedback strength, the ice-albedo feedback for high-latitude ice sheets is 14 times weaker than for the LGM–Holocene transition (for further illustration using a simple model, see SI Text). This reflects the notion that changes in glacial-interglacial ice cover per degree of warming were much larger than those expected for the future. Note that, although the discussion here illustrates changes for a single λ value, a suite of projections are provided using a wide range of λ values (Fig. 3). The moderate scenario may underestimate λ_2^{es} as several recent studies suggest that the future ice sheet response to warming could be stronger than previously thought (27, 33–35). Note, however, that uncertainties

in current estimates of ice mass changes for West Antarctica and the Antarctic Peninsula appear to remain large (36).

The feedback parameter for the combined effects of changes in vegetation, non-CO₂ GHGs, and low-latitude glaciers/ice caps in the moderate future scenario is $\lambda_1^{\text{es}} = 0.35 \text{ W}\cdot\text{m}^{-2}\cdot\text{K}^{-1}$. For comparison, $\sim 0.20 \text{ W}\cdot\text{m}^{-2}\cdot\text{K}^{-1}$ has been estimated for LGM–Holocene vegetation changes just in the latitude band 40°N–80°N, whereas corresponding estimates for changes in atmospheric CH₄ and N₂O are about $0.12 \text{ W}\cdot\text{m}^{-2}\cdot\text{K}^{-1}$ (3, 10). This gives a total of $\sim 0.32 \text{ W}\cdot\text{m}^{-2}\cdot\text{K}^{-1}$ for the combined effect of these two processes for the LGM–Holocene transition. The moderate future scenario assumes a similar value for λ_1^{es} but includes global vegetation changes (not restricted to 40°N–80°N) and effects of low-latitude glaciers/ice caps.

Conclusion

Regarding the legacy of anthropogenic GHG emissions (37), the main point of this study is that even if the fast-feedback sensitivity is no more than 3 K per CO₂ doubling, there will likely be additional long-term warming from slow climate feedbacks. Obviously, the projections presented here are subject to uncertainties (e.g., assessed via parameter variations; Fig. 3) and it is yet unknown whether high-end estimates of Earth system sensitivity are applicable to future projections. However, even low-end estimates of Earth system sensitivity such as for the Pliocene (3, 8) imply intensified and prolonged warming on millennial timescale (Figs. 2 and 3).

My results suggest a longer lifetime of human-induced future warming than previous studies (15, 38–41) (Fig. 2B). Note that the cited studies as well as the present study do not consider changes in orbital forcing. In extended model runs with low and moderate slow-feedback parameters (*Methods*), the temperature anomaly dropped to $1/e \sim 37\%$ of its maximum value after 23 and 165 ky for total emissions of 1,500 and 5,000 Pg C, respectively. All model simulations presented here include sediment CaCO₃ dissolution and negative, long-term weathering feedbacks, which tend to reduce the atmospheric lifetime of fossil fuel CO₂ (*SI Text*). In summary, including a time-dependent climate sensitivity in the projections suggests enhanced future climate change due to slow feedbacks that could amplify the warming and increase the probability for large ice sheet melting and major sea level rise. Note that the sea level rise from deglaciation needs to be added to the sea level rise from thermal expansion (21).

Long-lived peak warming ($>10,000$ y) as suggested here is more consistent with, albeit shorter than the duration of large climate perturbations in the past associated with massive carbon release such as the Paleocene–Eocene Thermal Maximum (PETM) (7, 42, 43). The PETM is considered the best analog for anthropogenic carbon input and independent dating techniques suggest a PETM main phase duration of intense warming of $>50,000$ y (44). One hypothesis for the longevity of the PETM warming involves additional carbon release from various reservoirs, mobilized as a feedback to the initial warming (45). If the present/future carbon cycle operates in a similar fashion, future warming could be more intense and longer lasting than previously thought.

Methods

The carbon cycle model LOSCAR has been used and tested in a number of earlier studies (e.g., refs. 7, 23, 46). For additional information on the use of

LOSCAR in the present study and model parameterizations, see *SI Text*. Below, the slow-feedback parameters are described, which are subject to uncertainties. The effect of these uncertainties on the results presented here is examined by varying the slow-feedback parameters over their likely range (Fig. 3).

Slow Feedbacks. The slow feedbacks include [1] combined effects of changes in vegetation, non-CO₂ GHGs, low-latitude glaciers/ice caps (λ_1^{es}), and [2] high-latitude ice sheets (λ_2^{es}). Changes in vegetation may occur over timescales ranging from decades to millennia (15, 47). For the effects combined under item [1], the response time τ_1 is taken as 200 y, whereas τ_2 is set to 5,000 y (for use of τ_j , see Eq. 6). The corresponding λ values are constrained as follows (Eq. 3). For the last glacial cycle, λ values for vegetation alone (only latitude band 40°N–80°N) and ice sheets have been estimated at ~ 0.20 and $\sim 0.70 \text{ W}\cdot\text{m}^{-2}\cdot\text{K}^{-1}$, respectively (3, 10). However, changes in glacial ice cover were much larger than expected for the future and hence the corresponding λ is considered an overestimate in the context of anthropogenic warming. The lower bound of the sum $\lambda_1^{\text{es}} + \lambda_2^{\text{es}}$ may be constrained by estimates of Earth system sensitivity at the lower end, $S_{2x}^{\text{es}} \simeq 4.0 \text{ K}$ (3, 8), yielding $\lambda_1^{\text{es}} + \lambda_2^{\text{es}} = 0.30 \text{ W}\cdot\text{m}^{-2}\cdot\text{K}^{-1}$. High estimates are $S_{2x}^{\text{es}} \simeq 9.7 \text{ K}$ (3, 10), which, again, applies to the last glacial cycle and represents an overestimate with regard to future climate change. Estimates from periods with relatively small (or no) changes in ice cover such as the Pliocene or the PETM may be more appropriate for the near future (3, 7–9). For instance, the PETM represents the best paleo-analog for future carbon release as it involved massive carbon input and global warming within a few thousand years. High estimates for the PETM are $S_{2x}^{\text{es}} = 7.0\text{--}8.0 \text{ K}$ (3, 7), yielding $\lambda_1^{\text{es}} + \lambda_2^{\text{es}} = 0.70\text{--}0.77 \text{ W}\cdot\text{m}^{-2}\cdot\text{K}^{-1}$. However, the individual range of λ_2^{es} may be taken as $0\text{--}0.1 \text{ W}\cdot\text{m}^{-2}\cdot\text{K}^{-1}$, assuming future ice sheet changes to be very small [this is probably a conservative estimate, given recent observations of warming and ice loss in Greenland and Central West Antarctica (34, 35)]. Hence a likely range of $\lambda_1^{\text{es}} + \lambda_2^{\text{es}}$ is $0.30\text{--}0.60 \text{ W}\cdot\text{m}^{-2}\cdot\text{K}^{-1}$ (Fig. 3). Moderate values for the slow-feedback parameters ($\lambda_{1,2}^{\text{es}}$; $\tau_{1,2}$) with units ($\text{W}\cdot\text{m}^{-2}\cdot\text{K}^{-1}$; y) are (0.35; 200) and (0.05; 5000) (Fig. 1). Note that λ values may also depend on the type of forcing and the background climate state (3, 25), which is however not well understood at present.

Slow Feedback Coefficients. The $c_j(t)$ in Eq. 3 could be chosen to increase smoothly from 0 to 1 over the response time of the slow processes. More generally, the delayed onset of the slow processes may be viewed as a lagged response to an average, past ΔT and hence the $c_j(t)$ may be tied to the integrated past temperature change ($\overline{\Delta T}$). For instance, for delayed feedbacks, an equation analog to Eq. 1 may be written as:

$$\Delta T = \Lambda_0^{-1} \left(\Delta R_f + \sum \lambda_j \overline{\Delta T}_j \right), \quad [5]$$

where

$$\overline{\Delta T}_j = (2\tau_j)^{-1} \int_{t-2\tau_j}^t \Delta T(t') dt' \quad [6]$$

and τ_j is the response time (delay) of process j . The $c_j(t)$ are then defined by $\overline{\Delta T}_j = c_j(t) \Delta T$, $\Delta T \neq 0$. In this case, the $c_j(t)$ and hence $S(t)$ (Eq. 3) are not known a priori but depend on the evolution of ΔT . Numerically, this is a nonissue as the $c_j(t)$ can be computed from ΔT at previous time steps. Eq. 6 was used here to calculate $\overline{\Delta T}_j$ and $c_j(t)$ for the slow processes. For simplicity, $\overline{\Delta T} = \Delta T$ was assumed for the fast processes.

ACKNOWLEDGMENTS. I thank the organizers of the workshop on Paleoclimate Sensitivity held in March 2011 in Amsterdam for putting together a great meeting, which prompted me to think about this problem. I also thank the editor and three anonymous reviewers for their constructive comments.

- Charney JG, et al. (1979) *Carbon Dioxide and Climate: A Scientific Assessment* (National Academy of Sciences, Washington, DC).
- Bony S, et al. (2006) How well do we understand and evaluate climate change feedback processes? *J Clim* 19:3445–3482.
- Rohling EJ, et al. (2012) Making sense of palaeoclimate sensitivity. *Nature* 491(7426): 683–691, 10.1038/nature11574.
- Intergovernmental Panel on Climate Change (2001) *Climate Change 2001: The Scientific Basis*, eds Houghton JT, et al. (Cambridge Univ Press, Cambridge, UK).
- Dufresne J-L, Bony S (2008) An assessment of the primary sources of spread of global warming estimates from coupled atmosphere ocean models. *J Clim* 21:5135–5144.
- Roe G (2009) Feedbacks, timescales, and seeing red. *Annu Rev Earth Planet Sci* 37:93–115.
- Zeebe RE, Zachos JC, Dickens GR (2009) Carbon dioxide forcing alone insufficient to explain Palaeocene-Eocene Thermal Maximum warming. *Nat Geosci* 2:576–580, 10.1038/ngeo578.
- Lunt DJ, et al. (2010) Earth system sensitivity inferred from Pliocene modelling and data. *Nat Geosci* 3:60–64.
- Pagani M, Liu Z, LaRiviere J, Ravelo AC (2010) High Earth-system climate sensitivity determined from Pliocene carbon dioxide concentrations. *Nat Geosci* 3:27–30, 10.1038/ngeo724.

10. Köhler P, et al. (2010) What caused Earth's temperature variations during the last 800,000 years? Data-based evidence on radiative forcing and constraints on climate sensitivity. *Quat Sci Rev* 29:129–145.
11. Zeebe RE (2011) Where are you heading Earth? *Nat Geosci* 4:416–417.
12. Previdi M, et al. (2013) Climate sensitivity in the Anthropocene. *Q J R Meteorol Soc* 139(674):1121–1131.
13. Hansen J, et al. (1984) Climate sensitivity: Analysis of feedback mechanisms. *Climate Processes and Climate Sensitivity*, AGU Geophysical Monograph Series, eds Hansen JE, Takahashi T (American Geophysical Union, Washington, DC), Vol 29, pp 130–163.
14. Myhre G, Highwood EJ, Shine KP, Stordal F (1998) New estimates of radiative forcing due to well mixed greenhouse gases. *Geophys Res Lett* 25:2715–2718.
15. Intergovernmental Panel on Climate Change (2007) *Climate Change 2007: The Physical Science Basis*, eds Solomon S, et al. (Cambridge Univ Press, Cambridge, UK).
16. Watterson IG (2000) Interpretation of simulated global warming using a simple model. *J Clim* 13:202–215.
17. Williams KD, Ingram WJ, Gregory JM (2008) Time variation of effective climate sensitivity in GCMs. *J Clim* 21:5076–5090.
18. Senior CA, Mitchell JFB (2000) The time-dependence of climate sensitivity. *Geophys Res Lett* 27:2685–2688.
19. Gregory JM, Forster PM (2008) Transient climate response estimated from radiative forcing and observed temperature change. *J Geophys Res* 113(D12):D23105.
20. Hansen J, Sato M, Kharecha P, von Schuckmann K (2011) Earth's energy imbalance and implications. *Atmos Chem Phys* 11:13421–13449.
21. Solomon S, Plattner G-K, Knutti R, Friedlingstein P (2009) Irreversible climate change due to carbon dioxide emissions. *Proc Natl Acad Sci USA* 106(6):1704–1709.
22. Roe GH, Baker MB (2007) Why is climate sensitivity so unpredictable? *Science* 318(5850):629–632.
23. Zeebe RE (2012) LOSCAR: Long-term Ocean-atmosphere-Sediment Carbon cycle Reservoir Model v2.0.4. *Geosci Model Dev* 5:149–166.
24. Hansen J, et al. (1985) Climate response times: Dependence on climate sensitivity and ocean mixing. *Science* 229(4716):857–859.
25. Yoshimori M, Hargreaves JC, Annan JD, Yokohata T, Abe-Ouchi A (2011) Dependency of feedbacks on forcing and climate state in physics parameter ensembles. *J Clim* 24:6440–6455.
26. Gregory JM, Huybrechts P (2006) Ice-sheet contributions to future sea-level change. *Philos Trans A Math Phys Eng Sci* 364(1844):1709–1731.
27. Robinson A, Calov R, Ganopolski A (2012) Multistability and critical thresholds of the Greenland ice sheet. *Nat Clim Change* 2:429–432.
28. Peters GP, et al. (2012) Rapid growth in CO₂ emissions after the 2008–2009 global financial crisis. *Nat Clim Change* 2:2–4.
29. Solomon S, et al. (2010) Persistence of climate changes due to a range of greenhouse gases. *Proc Natl Acad Sci USA* 107(43):18354–18359.
30. Archer D, Buffett B, Brovkin V (2009) Ocean methane hydrates as a slow tipping point in the global carbon cycle. *Proc Natl Acad Sci USA* 106(49):20596–20601.
31. Archer D, Buffett B (2005) Time-dependent response of the global ocean clathrate reservoir to climatic and anthropogenic forcing. *Geochem Geophys Geosyst* 6:3002.
32. Duplessy JC, Roche DM, Kageyama M (2007) The deep ocean during the last interglacial period. *Science* 316(5821):89–91.
33. Joughin I, Alley RB, Holland DM (2012) Ice-sheet response to oceanic forcing. *Science* 338(6111):1172–1176.
34. Shepherd A, et al. (2012) A reconciled estimate of ice-sheet mass balance. *Science* 338(6111):1183–1189.
35. Bromwich DH, et al. (2013) Central West Antarctica among the most rapidly warming regions on Earth. *Nat Geosci* 6:139–145, 10.1038/ngeo1671.
36. Hanna E, et al. (2013) Ice-sheet mass balance and climate change. *Nature* 498(7452):51–59.
37. Tyrrell T, Shepherd JG, Castle S (2007) The long-term legacy of fossil fuels. *Tellus B Chem Phys Meteorol* 59:664–672.
38. Archer D (2005) Fate of fossil fuel CO₂ in geologic time. *J Geophys Res* 110(1012):C09S05, 10.1029/2004JC002625.
39. Eby M, et al. (2009) Lifetime of anthropogenic climate change: Millennial time scales of potential CO₂ and surface temperature perturbations. *J Clim* 22:2501–2511.
40. Shaffer G, Olsen SM, Pedersen JOP (2009) Long-term ocean oxygen depletion in response to carbon dioxide emissions from fossil fuels. *Nat Geosci* 2:105–109.
41. Meissner KJ, McNeil BJ, Eby M, Wiebe EC (2012) The importance of the terrestrial weathering feedback for multimillennial coral reef habitat recovery. *Global Biogeochem Cycles* 26:GB3017.
42. Dickens GR, O'Neil JR, Rea DK, Owen RM (1995) Dissociation of oceanic methane hydrate as a cause of the carbon isotope excursion at the end of the Paleocene. *Paleoceanography* 10:965–971.
43. Zachos JC, et al. (2005) Rapid acidification of the ocean during the Paleocene-Eocene thermal maximum. *Science* 308(5728):1611–1615.
44. Zeebe RE, Zachos JC (2013) Long-term legacy of massive carbon input to the Earth system: Anthropocene vs. Eocene. *Philos Trans R Soc Lond A*, 10.1098/rsta.2012.0006.
45. Zeebe RE (2013) What caused the long duration of the Paleocene-Eocene Thermal Maximum? *Paleoceanography*, 10.1002/palo.20039.
46. Zeebe RE, Zachos JC, Caldeira K, Tyrrell T (2008) Oceans. Carbon emissions and acidification. *Science* 321(5885):51–52, 10.1126/science.1159124.
47. Whitlock C, Bartlein PJ (1997) Vegetation and climate change in northwest America during the past 125 kyr. *Nature* 388:57–61.